

Interstitial boron in silicon: A negative- U system

J. R. Troxell* and G. D. Watkins

Department of Physics and Sherman Fairchild Laboratory, Lehigh University, Bethlehem, Pennsylvania 18015

(Received 26 November 1979)

An electrical level 0.45 eV below the conduction band is detected by deep-level-capacitance transient spectroscopy (DLTS) in boron-doped silicon irradiated at 4.2 K by 1.5-MeV electrons. This level is attributed to interstitial boron. Greatly enhanced annealing of the level is observed under minority-carrier injection in both n - and p -type material. A quadratic dependence of the annealing rate on the injected current density reveals that the process is a *Bourgoin* mechanism in which the defect migrates by jumping from one lattice configuration to another as the defect alternates its charge state between B_i^+ and B_i^- . Combining these results with published electron-paramagnetic-resonance information, it is proposed that interstitial boron is an example of an Anderson "negative- U " system, with a single donor state ($0/+$) at $\sim E_c - 0.15$ eV which is *above* the single acceptor state ($-/0$) at $E_c - 0.45$ eV detected in the DLTS experiments.

I. INTRODUCTION

Previous studies¹⁻⁴ using electron paramagnetic resonance (EPR) have demonstrated that irradiation of silicon by high-energy electrons at cryogenic temperatures serves to displace substitutional impurity boron atoms into an interstitial configuration with high efficiency. The mechanism for this is believed to involve long-range motion of the interstitial *silicon* atoms, which are produced in the primary damage event, with subsequent trapping by the substitutional boron which is, in turn, ejected into the interstitial site as the silicon atom takes its place. As a result, the dominant defects produced by 1-2 MeV electrons at 4.2 or 20.4 K in boron-doped p -type silicon are believed to be isolated vacancies and interstitial boron atoms, in roughly 1:1 concentration. An EPR spectrum Si-G28 has been identified with the neutral charge state of the interstitial boron, and a detailed study of its properties has been published.⁴

In this paper, using deep-level-capacitance transient spectroscopy (DLTS), we detect an electrical level 0.45 eV below the conduction band denoted $E(0.45)$, which we identify as arising from the isolated interstitial boron atom. This identification is achieved by detailed correlation with the published EPR results. In addition, we show that under minority-carrier injection conditions, the defect exhibits a significantly enhanced annealing rate, which may be athermal. By a detailed study of the phenomenon, we are able to conclude that it is migrating via a *Bourgoin* mechanism,⁵⁻⁷ in which it alternates between two lattice configurations, one the saddle point for migration of the other, as the defect alternates between B_i^+ and B_i^- due to the capture of majority and minority carriers. Finally, we discuss the implications of

these results to the electronic structure of the defect. We propose that the $E(0.45)$ level is an *acceptor* state *below* a donor state at $\sim E_c - 0.15$ eV, thus providing an example of an Anderson "negative- U " system.⁸

II. EXPERIMENTAL PROCEDURE

For studies in n -type material, p^+n diodes were fabricated in the following manner: Wafers (~ 15 mil) were sliced from pulled n -type partially counterdoped silicon material that had been doped in growth with 3×10^{16} cm⁻³ phosphorus and 1×10^{16} cm⁻³ boron. (This is the same bulk material that had been used for the EPR studies in n -type material.⁴) Following polishing, p^+n mesa junctions were fabricated on the wafers using a spin-on boron diffusion source. Aluminum was deposited on both faces of the wafers and the diode structures were defined with black wax. The surrounding silicon and aluminum were then removed by etching with nitric acid (HF:acetic:HNO₃; 1:1:6). Samples were then diced and mounted on TO-12 headers using a silver-laden conductive epoxy, and contacted by ultrasonic bonding of 1-mil aluminum wires.

The n^+p diodes used for the p -type studies were supplied to us by Dr. A. O. Ewvaraye of the General Electric Research and Development Center. They had been fabricated on two-inch Monsanto-Monex wafers containing 1.5×10^{16} cm⁻³ boron by conventional photolithography and phosphorus diffusion techniques.

Irradiations were performed *in situ* with 1.5-MeV electrons from the Lehigh Van de Graaff accelerator, using an Air Products Cryo-Tip to maintain sample temperatures near 4.2 K. Total fluences were $\sim 1 \times 10^{16}$ electrons/cm².

Samples were studied using a deep-level-capaci-

tance transient spectrometer of the type described by Lang.⁹ The spectrometer employed a capacitance bridge operating at 10 MHz and transient detection by means of a double boxcar signal averager. The spectrometer was calibrated using a circuit which is described elsewhere.¹⁰

Annealing studies were performed by monitoring the amplitudes of the DLTS signals between anneals performed *in situ* in the Cryo-Tip. Isothermal recovery was found to give a simple exponential decay (or growth) versus time, characteristic of first-order reaction kinetics. In many cases the signals were strong enough that the annealing time constant τ could be estimated under several different sets of conditions (temperature, bias, injection level, etc.) on a single sample before the recovery had gone to completion.

III. EXPERIMENTAL RESULTS

A typical defect spectrum observed in the *n*-type partially counterdoped material after irradiation at 4.2 K and annealing to 100 K¹¹ is shown in Fig. 1. The $E(0.16)$ level has been observed in most DLTS studies of *n*-type silicon and arises from a vacancy trapped by interstitial oxygen, the A center.¹² Similarly, the $E(0.43)$ level arises from the phosphorus-vacancy pair, which has also been studied in detail.¹³ The dominant level, however, at $E(0.45)$ has not been previously reported. It is found to have an electron emission rate of

$$e_s = 6.2 \times 10^{13} \exp(-0.49 \pm 0.02 \text{ eV}/kT) \text{ sec}^{-1}. \quad (1)$$

The electron emission activation energy $E_s(0.49 \text{ eV})$ may then be related to the defect energy-level position by using the standard result of detailed balance between carrier capture and emission processes¹⁴:

$$e_s = X_s \sigma_s \langle v_s \rangle N_c \exp[-(E_c - E_T)/kT], \quad (2)$$

where E_T is the defect energy-level position, N_c is the effective-mass density of states within the conduction band, $\langle v_s \rangle$ is the electron thermal velocity within the lattice, and σ_s is the electron-capture cross section for the defect. X_s is a multiplication factor which originates from the change in entropy taking place when a carrier is excited from the defect. In general, the temperature dependence of $\langle v_s \rangle N_c$ is quadratic, while the dependence of σ_s may vary considerably.

We find $\sigma_s \geq 10^{-16} \text{ cm}^2$, with no evidence of a temperature dependence. Thus we estimate the energy level of the defect to be

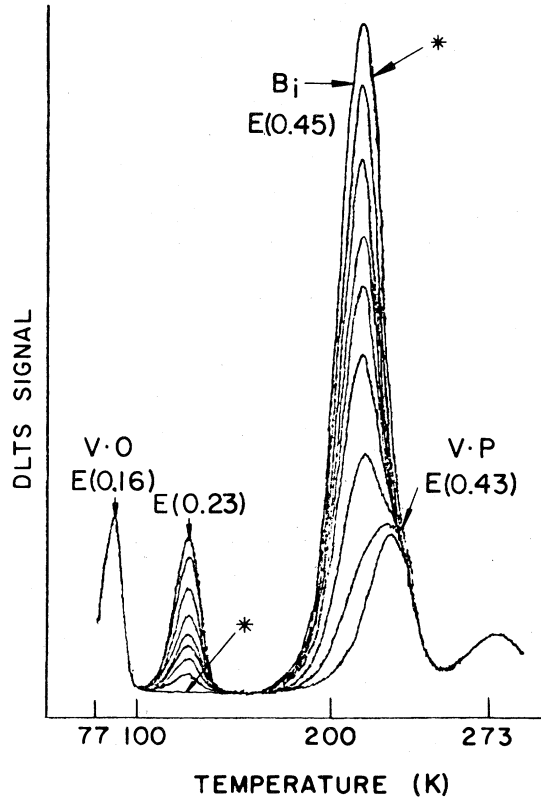


FIG. 1. DLTS spectrum of *n*-type (phosphorus $3 \times 10^{16} \text{ cm}^{-3}$) silicon partially counterdoped with boron ($1 \times 10^{16} \text{ cm}^{-3}$) after 1.5-MeV electron irradiation at 4.2 and 100 K anneal (*). Shown also are successive anneals at 240 K which reveal the emergence of a new level at $E(0.23)$ as the dominant $E(0.45)$ level disappears and the presence of a level at $E(0.43)$ originally masked by the strong $E(0.45)$ signal. [The $E(0.43)$ peak appears at a higher temperature than that for $E(0.45)$ because of a lower preexponential factor in its emission rate.]

$$E_c - E_T = E_s - 2kT = 0.49 \pm 0.02 - 0.04 \\ = 0.45 \pm 0.02 \text{ eV},$$

where the $2kT$ term corrects for the T^2 dependence of $\langle v_s \rangle N_c$. Under zero-biased (shorted) junction conditions this defect level is stable to ~ 240 K. Its disappearance is correlated with the growth of a defect level at $E_c - 0.23 \text{ eV}$ (Fig. 1). The annealing rate τ_{zb}^{-1} under zero-bias conditions is found to be (solid line, Fig. 2),

$$\tau_{zb}^{-1} = 2.5 \times 10^{10} \exp(-0.63 \pm 0.03 \text{ eV}/kT) \text{ sec}^{-1}. \quad (3)$$

When a reverse bias is applied to the junction during annealing, the rate τ_{rb}^{-1} is substantially reduced:

$$\tau_{rb}^{-1} = 5 \times 10^7 \exp(-0.60 \pm 0.05 \text{ eV}/kT) \text{ sec}^{-1}. \quad (4)$$

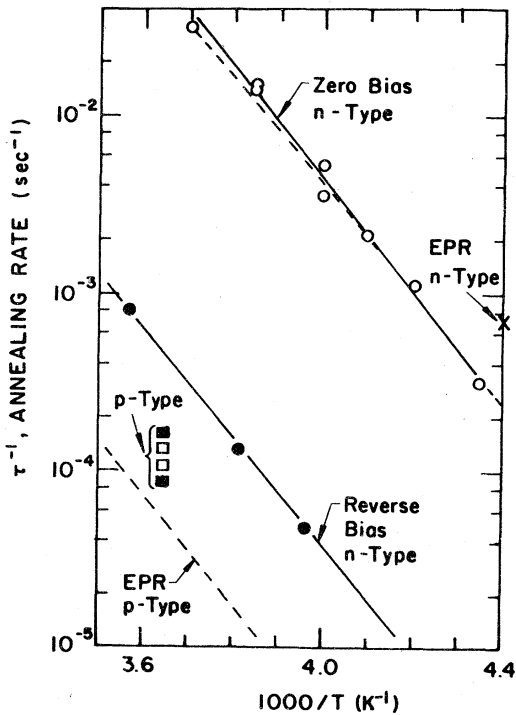


FIG. 2. Annealing kinetics for the loss of the $E(0.45)$ level under zero (\circ) and reverse bias (\bullet) in n -type material. Also shown is the growth of the $E(0.23)$ level in p -type material under zero (\square) and reverse (\blacksquare) bias. Shown for comparison are EPR results for interstitial boron. The dashed curve is theoretically predicted for the n -type zero-bias anneal assuming a thermally stimulated Bourgoin mechanism (see text).

The growth of the $E(0.23)$ level also matches the $E(0.45)$ annealing rate under reverse-bias conditions.

In p -type material, we do not detect the $E(0.45)$ level as a minority-carrier trap (forward bias during the trap-filling pulse). The $E(0.23)$ level, however, is observed. Therefore, we can monitor the annealing process in the p -type material by studying the growth of the $E(0.23)$ level. Results of limited studies of this type are also shown in Fig. 2. No difference was detected for zero or reverse bias.

Also shown in Fig. 2 is annealing data for the interstitial boron Si-G28 spectrum from EPR studies. The results in p -type silicon have been previously published.⁴ The single point for n -type material is from unpublished results.

The $E(0.45)$ level exhibits substantially enhanced annealing under minority-carrier (hole) injection conditions. Annealing data for n -type counterdoped samples under forward-bias junction conditions are shown in Fig. 3. The previous results in the absence of minority-carrier injection (Fig. 2) are also shown for comparison on the com-

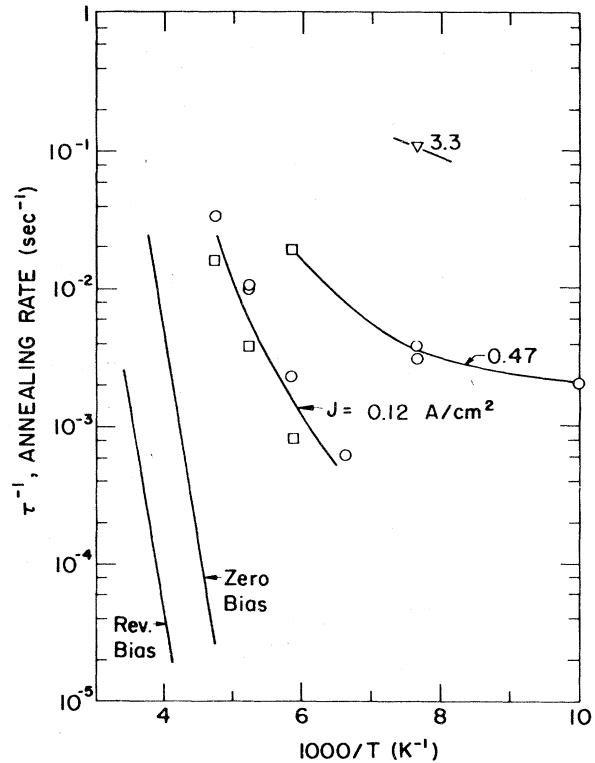


FIG. 3. Annealing kinetics under injection conditions for the $E(0.45)$ level in counterdoped n -type material. (\circ , \square , ∇ refer to data taken on different samples.) Points connected by the curves were measured for the injection current density indicated. Also shown for comparison are the zero- and reverse-bias results from Fig. 2.

pressed scale of Fig. 3. As was the case in the absence of minority-carrier injection, the growth of the $E(0.23)$ level again is observed to correlate with the $E(0.45)$ level disappearance. Thus, although the $E(0.45)$ level cannot be detected in p -type material, we may again monitor the annealing kinetics in p -type material by the growth of the $E(0.23)$ level. The minority-carrier (electrons in this case) injection-enhanced annealing kinetics in p -type material are then given by Fig. 4.

The dependence of the annealing rate upon injection-current density is shown in Fig. 5. The annealing rate is seen to be roughly the same in both n - and p -type materials at a given injection level and to vary approximately quadratically with the injection-current density. No other level has been observed in either p - or n -type materials that can be correlated with interstitial boron.

IV. PREVIOUS EPR RESULTS⁴

In both p - and n -type silicon, the interstitial boron Si-G28 spectrum must be generated with

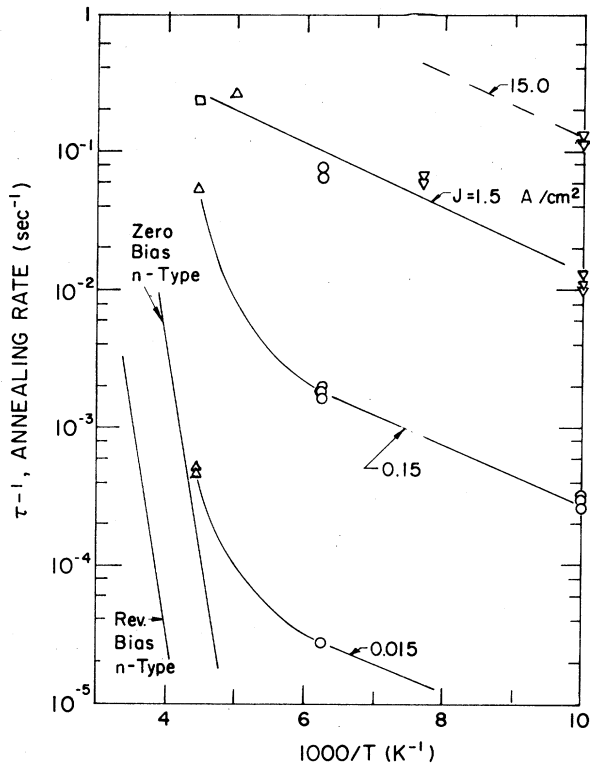


FIG. 4. Annealing kinetics for the growth of the $E(0.23)$ level in p -type material under minority-carrier injection conditions. (\circ , \square , ∇ , Δ refer to data taken on different samples.) Points connected by the curves were measured for the injection current density indicated. Shown for comparison are the zero- and reverse-bias results in n -type material.

near-band-gap light. The spectrum, normally observed at 20.4 K, is not stable in either low resistivity n - or p -type silicon, but decays when the light is turned off. As a result, it was concluded that two energy levels (or three charge states) are associated with interstitial boron. Since the defect is observed in the neutral charge state, these would be single donor ($0/+$) and single acceptor levels ($-/0$), respectively.¹⁵ In p -type samples, made high resistivity by prolonged irradiation, the photo-produced spectrum is stable in the dark to ~ 50 K. The decay at this temperature was interpreted as thermal excitation of a trapped electron from the donor level to the conduction band, indicating an energy level for the donor state near $\sim E_c - 0.15$ eV.

The anisotropy of the observed EPR spectrum revealed that the neutral boron atom is not located in the normal tetrahedral or hexagonal interstitial site. Instead, the symmetry indicated a small distortion from a lattice position otherwise reflecting a strong $\langle 111 \rangle$ axial crystalline environment. Three possible models were suggested: (a)

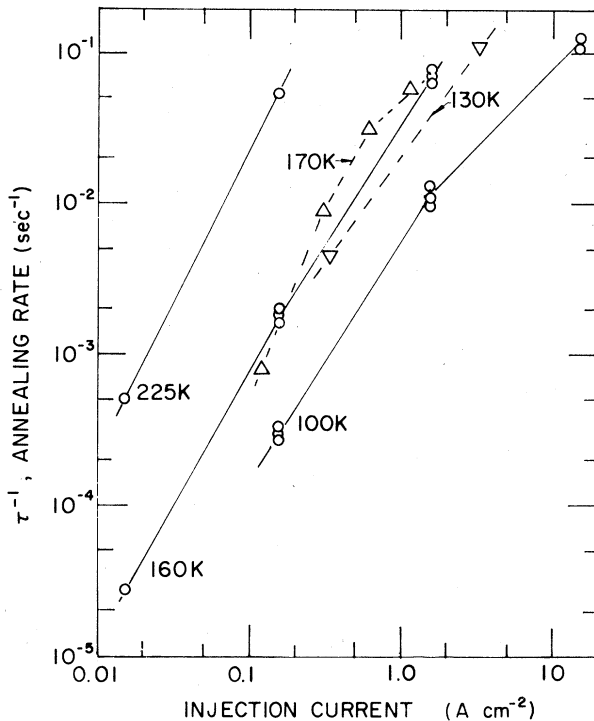


FIG. 5. Annealing rate versus injection current density for p -type (solid lines) and n -type (dashed lines) materials.

a bent-bond Si-B-Si interstitialcy, in which the boron squeezes in between two normally bonded silicon atoms, (b) a bent-bond Si-Si-B configuration, and (c) a distortion out of the normal hexagonal interstitial site. Most of the available evidence favored model (a), but it was not possible to rule out any of the three models. Evidence was also cited to indicate that in the positive charge state, the boron ion relaxes into the pure $\langle 111 \rangle$ configuration.

The kinetics for the interstitial boron reorientation⁴ rate τ^{-1} from one $\langle 111 \rangle$ axis to another were determined to be

$$\tau^{-1} = 5 \times 10^{12} \exp(-0.60 \pm 0.05 \text{ eV}/kT) \text{ sec}^{-1}. \quad (5)$$

Annealing kinetics were also studied for the disappearance of the spectrum in p -type material, giving

$$\tau^{-1} = 5.3 \times 10^6 \exp(-0.60 \text{ eV}/kT) \text{ sec}^{-1}. \quad (6)$$

The identical activation energy for the two processes suggests that defect reorientation is equivalent to migration. The difference in the preexponential terms is consistent with long-range defect migration, which would require $\sim 10^6$ defect jumps (or reorientations) before being trapped by some other defect.

It was also observed that $\langle 111 \rangle$ axis reorientation could be produced at 4.2 or 20.4 K by minority-carrier injection as generated by light or by high-energy electron irradiation. If reorientation is equivalent to a one-jump migrational process, ionization-enhanced annealing should also be occurring at these temperatures. An attempt to test this by prolonged injection was inconclusive.

V. DISCUSSION

A. General

The $E(0.45)$ level is detected only following electron irradiation of silicon which contains a substantial quantity of boron. In n -type silicon with $\sim 1 \times 10^{16}$ boron, it is the dominant level observed. Under zero bias, this defect level anneals near 240 K with kinetics similar to that observed for the anneal of interstitial boron in previous EPR studies in the same material (Fig. 2). Although the $E(0.45)$ level itself is detected only in n -type doped silicon, its disappearance near 240 K is accompanied by the growth of a level at $E(0.23)$, which is detected in both n - and p -type electron-irradiated silicon containing boron. This level has previously been detected in irradiated p -type boron-doped material and tentatively identified with boron.^{12,16} We therefore identify the $E(0.45)$ level as a level of interstitial boron.

Under zero-junction-bias conditions the Fermi level is above the $E(0.45)$ defect level, while under reverse-bias conditions the Fermi level is nominally at mid-gap, below the $E(0.45)$ defect level. Thus the variation in junction-bias conditions results in a change of the equilibrium charge state of the defect, providing an explanation for the large change in the annealing kinetics observed for the defect in the two cases (Fig. 2). Such charge-state effects have been reported for several radiation-induced defects in silicon.^{2,3,13,17} It should be noted, however, that in most cases the variation in annealing kinetics has resulted from a variation in annealing activation energies. In the case of the $E(0.45)$ level, however, the observed difference in annealing rates appears to result primarily from a variation in the preexponential term [(Eqs. (3) and (4))]. We will return to this point later in the discussion.

In all of the annealing studies of n -type material, a direct correlation was found between the disappearance of the $E(0.45)$ level and the growth of the $E(0.23)$ level. We conclude, therefore, that the annealing process can also be monitored in p -type material by the growth of the $E(0.23)$ level, even though the $E(0.45)$ level cannot be directly detected. Our annealing studies in p -type samples yield similar rates under zero and reverse bias,

which also match approximately the n -type results under reverse-bias conditions (Fig. 2). These annealing kinetics, in turn, agree reasonably well with those measured for interstitial boron from EPR studies in p -type silicon given in Eq. (6) and also shown in the figure. (The agreement is considered satisfactory because the three different sets of data are on different samples. The EPR results were on floating zone samples, the n -type diodes were from pulled crystals, and the p -type diodes, though of low initial oxygen content, undoubtedly had oxygen incorporated during the phosphorus diffusion. Also, the samples used for EPR studies were more heavily irradiated.)

We conclude tentatively, therefore, that no further defect charge-state changes occur as the Fermi level moves through the lower half of the silicon band gap, which in turn means that interstitial boron does not introduce any additional levels below the $E_c - 0.45$ eV level. This is consistent with our failure to detect any levels in p -type silicon which can be correlated with interstitial boron.

B. Injection-enhanced annealing

Under minority-carrier injection conditions (Figs. 3 and 4), a large enhancement in the defect annealing rate is observed. For sample temperatures ≥ 150 K, substantial temperature dependence for the annealing rate remains. At lower temperatures, however, the rates become relatively insensitive to temperature. At a current density J of 1.5 A cm^{-2} in the p -type material, the annealing rate τ^{-1} in the region down to 100 K can be estimated roughly to be

$$\tau^{-1} = 3 \exp(-0.05 \pm 0.03 \text{ eV}/kT) \text{ sec}^{-1}, \quad (7)$$

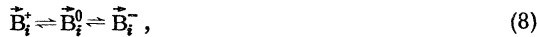
nearly athermal in nature.

It is interesting to note that within the experimental error of the data, the injection-enhanced annealing rates are the same in both p - and n -type samples at comparable currents and temperatures (Fig. 5). Also, in neither case does the annealing rate appear to saturate. Thus, we may conclude that for these current densities ($\approx 1 \text{ A/cm}^2$) the enhanced annealing rate is being limited by the injected minority-carrier capture rate in both n -type and p -type samples. The equality of the rates and the absence of rate saturation with increasing minority-carrier concentrations suggest that the relevant electron and hole-capture cross sections at the defect are of comparable magnitude.

This observation is consistent with the inability to detect the $E(0.45)$ level in p -type material as a minority-carrier trap. The comparable capture cross sections would prevent the detection of the

level because under injection conditions, majority carriers are always present in excess of minority carriers. It is not possible under such conditions to get a significant number of defects into the minority-carrier-related charge state, and thus it is not possible to detect the defect level.

The approximate quadratic dependence upon injected current, Fig. 5, is unusual and has not been observed to our knowledge in any other example of an injection-enhanced reaction in solids. It suggests a two-step process, the rate of each being proportional to the injected minority-carrier density. This, in turn, indicates that the process requires the capture of *two* electrons in *p*-type material, *two* holes in *n*-type material. We may conclude, therefore, that the enhanced migrational process involves the alternation between charge states of the defect that differ by two electronic charges. Since from EPR studies it was concluded that \tilde{B}_i^+ , \tilde{B}_i^0 , and \tilde{B}_i^- exist, this suggests the process



where a one-jump motion occurs *only* if the complete cycle, B_i^+ to B_i^- and return, has taken place.

Including both electron and hole capture and emission processes, the complete charge-state-change cycle rate is easily shown to be given by

$$\begin{aligned} \nu &= f^-(c_h^- + e_a^-) \frac{c_h^0 + e_a^0}{c_h^0 + e_a^0 + c_a^0 + e_h^0} \\ &= f^+(c_a^+ + e_h^+) \frac{c_a^0 + e_h^0}{c_h^0 + e_a^0 + c_a^0 + e_h^0}, \end{aligned} \quad (9)$$

where e_a^i , e_h^i , c_a^i , c_h^i , and f^i are the electron-emission rate, hole-emission rate, electron-capture rate, hole-capture rate, and fractional concentration for the *i*th charge state, respectively.

In *p*-type material, emission processes can be neglected, and at low injection levels where the electron concentration (*n*) is much less than the majority-hole concentration (*p*), $c_h^i > c_a^i$. This leads to a quadratic dependence on *n*,

$$\nu_p \sim f^+ c_a^+ \frac{c_a^0}{c_h^0} = \frac{\sigma_a^+ \sigma_a^0 \langle v_a \rangle^2}{\sigma_h^0 \langle v_h \rangle p_0} n^2. \quad (10)$$

Here σ_a^i , σ_h^i are the electron- and hole-capture cross sections for the *i*th charge state and $\langle v_a \rangle$ and $\langle v_h \rangle$, the average thermal velocities for conduction electrons and holes, respectively. In (10) we have used the fact that for $n \ll p$, $f^+ \sim 1$ and $p \sim p_0$, the majority-carrier concentration in the absence of injection.

Similarly, in *n*-type material with $p \ll n$ and the additional restriction $e_a^0 < c_h^0$, a quadratic dependence on *p* results:

$$\nu_n \sim f^- c_h^- \frac{c_h^0}{c_a^0} \sim \frac{\sigma_h^- \sigma_h^0 \langle v_h \rangle^2}{\sigma_a^0 \langle v_a \rangle n_0} p^2, \quad (11)$$

where in this case $f^- \sim 1$ and $n \sim n_0$. With $\langle v_h \rangle \sim \langle v_a \rangle$, and $p_0 \sim n_0$, the equality of rates in the *n*- and *p*-type materials at comparable injection levels now implies

$$\frac{\sigma_a^0 \sigma_a^+}{\sigma_h^0} \sim \frac{\sigma_h^- \sigma_h^0}{\sigma_a^0}. \quad (12)$$

The magnitude of the observed annealing rate is also reasonably accounted for by Eqs. (10) and (11). Following Henry *et al.*,¹⁸ we may estimate the minority-carrier (hole) concentration in *n*-type material under forward-bias conditions by

$$p = (\gamma J/q)(t_p/kT\mu_p)^{1/2}, \quad (13)$$

where γ is an injection efficiency (assumed to be 0.5), q is the electronic charge, t_p is the minority-carrier lifetime, and μ_p is the hole mobility (~ 400 cm² V⁻¹ sec⁻¹). For a current density $J = 0.47$ A/cm², and $T = 100$ K, we obtain

$$p \sim 8 \times 10^{17} t_p^{1/2} \text{ cm}^{-3}. \quad (14)$$

Assuming $\sim 10^6$ defect jumps before the defect is trapped, the observed annealing rate 2×10^{-3} sec⁻¹ (Fig. 3) would correspond to a one-jump rate of $\sim 2 \times 10^3$ sec⁻¹ at 100 K. With $\sigma_h^- \sim \sigma_h^0 \sim \sigma_a^0 \sim 10^{-16}$ cm², $n_0 = 2 \times 10^{16}$ cm⁻³, and $\langle v_a \rangle \sim \langle v_h \rangle \sim 10^7$ cm/sec, Eqs. (11) and (14) give a one-cycle charge-state change rate $\nu = 2 \times 10^3$ sec⁻¹ for a minority-carrier lifetime $t_p \sim 10^{-7}$ sec. This is a reasonable value for irradiated material. With this, the minority-carrier concentration, Eq. (14), is 3×10^{14} cm⁻³, a factor of a hundred lower than the majority-carrier concentration in agreement with the assumptions leading to Eqs. (10) and (11).

The fact that the process requires the complete cycle appears to rule out an energy release mechanism^{6,19} for the motion. In this mechanism, the energy release upon capture of a carrier is converted to kinetic energy of the atom to assist it over its migrational barrier. This process, which has been identified for a few specific defects in semiconductors,¹⁹⁻²⁴ would occur at a particular capture process in the chain, Eq. (8), and therefore could lead to quadratic dependence upon injection current in one conductivity type, but not the other.

The requirement of the complete cycle implies a "saddle-point" (or Bourgoin⁵) mechanism. In this mechanism, the stable configuration for B_i^- would be the saddle point for migration of B_i^+ , and, vice versa, the conversion from one to the other and back, therefore, providing a diffusional jump. The fact that neither the $B_i^+ \rightleftharpoons B_i^0$ nor the $B_i^0 \rightleftharpoons B_i^-$ conversion accomplishes the jump by itself implies

that B_i^0 is an intermediate configuration, "halfway between" two specific B_i^+ and B_i^- configurations.

The EPR studies⁴ provide a striking confirmation of this idea. The EPR spectrum for B_i^0 reveals two distinct symmetry lowering features. One reflects a $\langle 111 \rangle$ axial crystalline environment which is retained in the $B_i^0 \rightleftharpoons B_i^+$ conversion and is therefore common also to the B_i^+ configuration. The other is a distortion in a $\{110\}$ plane away from the $\langle 111 \rangle$ axis, the memory of which is lost in the $B_i^0 \rightleftharpoons B_i^+$ conversion. From this it was concluded that B_i^+ is in a pure $\langle 111 \rangle$ axial configuration and in the conversion to B_i^0 it "puckers" out into one of the six possible off-axis directions provided by the three $\{110\}$ planes containing this axis. It is still attached to its original $\langle 111 \rangle$ axis and the $B_i^0 \rightleftharpoons B_i^+$ conversion, therefore, allows no net translational movement in the lattice. We may interpret the puckering now to reveal the intermediate step, presumably completed in the $B_i^0 \rightleftharpoons B_i^-$ conversion to a different high-symmetry configuration, from which other $\langle 111 \rangle$ B_i^+ configurations are accessible.

Figure 6 illustrates a possible microscopic model for the process. In (a), the stable configuration for B_i^+ is a $\langle 111 \rangle$ bond-centered interstitialcy,

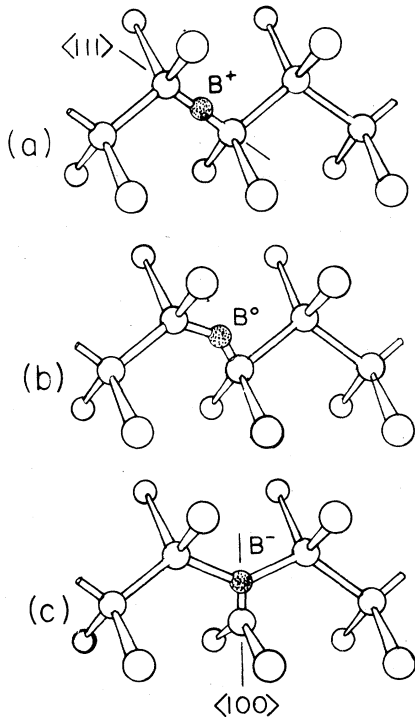


FIG. 6. Possible model for Bourgoin migration of interstitial boron in silicon: (a) B_i^+ is in a bond-centered interstitialcy position; (b) B_i^0 , seen in EPR, puckers out from the bond-centered position into an intermediate position in the $\{110\}$ plane; (c) B_i^- is in a split- $\langle 100 \rangle$ interstitialcy configuration.

the boron ion nestling between two normally bonded silicon atoms. In (c) the stable configuration for B_i^- is a $\langle 100 \rangle$ -split interstitial, the boron ion forming a $\langle 100 \rangle$ -oriented B-Si dumbbell which occupies a single lattice site. These configurations have been predicted to be stable ones for interstitial atoms in the diamond lattice from extended Hückel theory cluster calculations²⁵⁻²⁷ and are, therefore, reasonable models. (Additional confirmation comes from EPR studies which reveal a split $\langle 100 \rangle$ character for interstitial C^{*} in silicon.²⁸) In (b) the configuration of B_i^0 is intermediate between the two other configurations, the off-axis distortion reflecting the specific $\langle 100 \rangle$ -oriented dumbbell from which it has originated and/or to which it must go in the $B_i^0 \rightleftharpoons B_i^-$ conversion. From the B_i^+ configuration, the six equally possible distortions correspond to intermediate motion toward three possible $\langle 100 \rangle$ dumbbell orientations for B_i^- on each of two possible atomic sites. From each B_i^- dumbbell configuration, two equally probable motions are possible: one a return toward the original B_i^+ position, the other toward a new $\langle 111 \rangle$ bond center position. Thus migrational diffusion becomes possible in the complete $B_i^+ \rightleftharpoons B_i^-$ cycle.

The configuration for B_i^0 in the figure is fully consistent with the EPR analysis and corresponds to model (a) presented in that work.⁴ It is not unique in microscopic detail, however, as previously pointed out. It remains possible also, for instance, to devise similar models for conversion between either of the other two suggested EPR models for B_i^+ (Si-Si-B interstitialcy or the hexagonal interstitial site), and either a $\langle 100 \rangle$ -split interstitial configuration for B_i^- or even B_i^+ in the tetrahedral interstitial site. Recent cluster calculations by Mainwood and Stoneham for diamond²⁹ using the complete neglect of differential overlap method have concluded, for instance, that the bond-centered configuration of Fig. 6 is energetically unfavorable compared either to the $\langle 100 \rangle$ split or hexagonal site, so the hexagonal-site model for B_i^+ must also be considered a viable possibility. In Figure 7 a possible hexagonal site $B_i^+ \leftrightarrow$ split- $\langle 100 \rangle$ B_i^- conversion is also sketched. Further EPR studies are planned to help distinguish these alternatives.

C. Electrical level structure

The EPR results and the injection-enhanced annealing both indicate the existence of three charge states, i.e., B_i^+ , B_i^0 , and B_i^- . We must, therefore, ask why only one level is seen in the DLTS studies. The EPR results indicated that the donor level ($0/+$) should be at $\sim E_a - 0.15$ eV, but

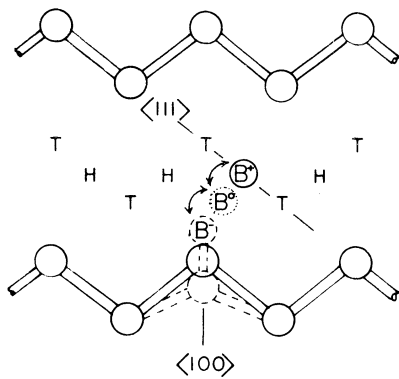


FIG. 7. Alternate model for Bourgoin migration in which conversion between B_i^+ in a hexagonal interstitial site and B_i^- in a split- $\langle 100 \rangle$ configuration (dashed lines) occurs. B_i^0 is in an intermediate position (dotted lines) which is also consistent with the EPR results. Shown are atoms and the interstitial tetrahedral (T) and hexagonal (H) sites in a $\{100\}$ plane.

no level shallower than the $E(0.45)$ level has been detected that could be associated with boron. (The DLTS studies should have detected a level at least as shallow as $E_c - 0.07$ eV.)

Figure 8 illustrates a proposed level structure that explains the observations. The donor level ($0/+$) is at $\sim E_c - 0.15$ eV, consistent with the EPR observations, and the $E_c - 0.45$ eV level is identified as the single acceptor ($-/0$) state. This represents an inversion of the usual order (for which the acceptor states lie above the donor states) and corresponds to a negative- U system as originally proposed by Anderson,⁸ and later expanded by Street and Mott,³² to explain anomalous diamagnetic behavior of defect states in the chalcogenide glasses.

In such a system, the B_i^0 state is only a *metastable* state, the reaction



lowering the energy of the system. In p -type material, the stable charge state is, therefore, B_i^+

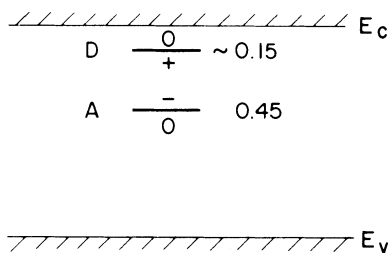


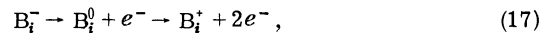
FIG. 8. Proposed electrical level structure for interstitial boron. The $E(0.45)$ level detected by DLTS is the single acceptor state (A) and the level at $\sim E_c - 0.15$ eV detected by EPR studies is the single donor state (D). This inverted order implies a negative- U system.

and in n -type is B_i^- . The EPR observation that B_i^0 is only observed after photoexcitation in n - or p -type material at temperatures below freezeout is therefore explained by this model. The metastable B_i^0 decay in high resistivity material, therefore, reflects the thermal ionization



locating the donor level at $\sim E_c - 0.15$ eV, consistent with the previous interpretation of the EPR results.

Normal DLTS studies will not detect this level because in filling the trap under zero bias, the defect captures two electrons and under reverse bias, it decays from B_i^- by thermally activated electron emission. This decay process,



is limited by the first ionization event which reflects the 0.45-eV level depth. At temperatures where this can be monitored, the second electron, being bound by only ~ 0.15 eV, follows immediately. In effect, then, only one DLTS peak will be observed, that reflecting the deeper acceptor level at $E(0.45)$.

If this is correct, an essential consequence is that two electrons are emitted for each ionization event, and each defect changes its charge state correspondingly by two electronic charges. In the DLTS experiment, it is the charge-state change of the defects in the depletion region that is being monitored, and the height of the peak is a direct measure of the total charge-state change in this region due to the ionization of the defect. If we knew the concentration of the interstitial boron defects by some other means, we could determine the charge-state change directly. Unfortunately, since the defects are produced by irradiation, the concentration is not well known.

We can, however, make an estimate another way. The accumulated evidence from low-temperature damage studies with ~ 1.5 -MeV electrons is that the principal damage products stable after a 4.2 or 20.4 K irradiation are equal concentrations of isolated vacancies and interstitial group III atoms.¹⁻⁴ In the studies described here, the interstitial atoms are boron. The mechanism for interstitial boron production is speculated to be highly efficient athermal ionization-enhanced migration of the primary interstitial silicon atom with subsequent trapping by substitutional boron to eject the boron into the interstitial site. The high cross section for interstitial trapping by boron (as opposed to oxygen, for instance) presumably reflects a long-range Coulomb attraction. On subsequent annealing to ~ 100 K in n -type material, the vacancies migrate and are trapped by

other defects.³ In our n -type counterdoped materials, the dominant traps should be oxygen to form the vacancy-oxygen pair (VO) at $E(0.16)$, and phosphorus to form the phosphorus-vacancy pair (VP) at $E(0.43)$. Both of the levels can be seen in Fig. 1, the VP pair being resolved cleanly as the interstitial boron anneals. Consistent with this, the dominant levels observed in Fig. 1 after annealing to 100 K are these three centers, the VO and VP pairs, and the $E(0.45)$ interstitial boron peak. As seen in the figure, the sum of the two vacancy-related peaks is almost exactly one-half that of the $E(0.45)$ peak. We find the relation to hold for all samples studied. We consider this strong evidence that the negative- U model illustrated in Fig. 8 is correct and the ionization being observed for interstitial boron is a double one.

This model also provides a possible explanation for the difference in the thermally activated annealing rates for zero and reverse bias in n -type silicon given by Eqs. (3) and (4). We pointed out earlier that the difference appeared to be primarily in the preexponential factor, an uncommon observation. Normally we expect a preexponential factor $\sim 10^7$, which reflects an $\sim 10^{13}$ characteristic vibrational attempt frequency divided by $\sim 10^6$, the number of single jumps required to encounter another defect before being trapped. The n -type reverse-bias result (and the corresponding results in p -type material), therefore, apparently represents the "normal" one, and the 0.60-eV activation energy presumably represents the energy barrier that the B_i^+ atom must surmount in order to make a diffusional jump.

In the case of the n -type zero-bias results, we must also consider the possible contribution of the Bourgoin charge-state alternation mechanism, Eq. (8), which results from thermally stimulated electron emission. Here the alternation cycle rate is given by Eq. (9) with all hole capture and emission terms set to zero:

$$\nu_n' \sim f^- e_e^- \alpha / (1 + \alpha), \quad (18)$$

where

$$\alpha = \frac{e_e^0}{c_e^0} = \frac{X_e^0 \sigma_e^+ N_c \exp(-E_{(0/+)} / kT)}{\sigma_e^0 n_0}. \quad (19)$$

With $X_e^0 \sim 1$, $\sigma_e^+ \sim \sigma_e^0$, $n_0 = 2 \times 10^{16} \text{ cm}^{-3}$, $f^- \sim 1$, $E_{(0/+)} = 0.15 \text{ eV}$, and³⁰

$$N_c = 2.1 \times 10^{19} (T/250)^{3/2} \text{ cm}^{-3},$$

these equations allow a direct estimate of ν_n' using the experimentally measured emission rate e_e^- from Eq. (1). In Fig. 2, the dashed curve is the calculated value ν_n' divided by 10^6 , to account for the number of jumps before trapping. The agreement is remarkable, both in the slope of the

curve (apparent activation energy) and its absolute magnitude. The close agreement for the magnitude is, of course, somewhat fortuitous, there being a number of uncertainties in cross sections, entropy factors, etc. However, it clearly illustrates that the thermally induced Bourgoin mechanism can account for the zero-bias annealing in n -type material.

The origin of the factor of $\sim 10^3$ increase in the preexponential factor observed for the n -type zero-bias annealing results, Eq. (3), can now be seen to come from the N_c/n_0 ratio in α , Eq. (19). As has been previously pointed out,³¹ this arises specifically because the process is a two-step one, the first of which requires a thermally induced charge-state change. In other systems where anomalously large preexponential terms are observed, the possibility of this type of contribution should, therefore, also be carefully considered.

Note added in proof. Under reverse bias, capture processes can be neglected, and Eq. (18) becomes $\nu_n' = f^- e_e^-$. With rapid short zero-bias pulses to keep $f^- \sim 1$, the thermally induced contribution to the Bourgoin annealing rate under reverse bias should therefore be increased by $(1 + \alpha)/\alpha$ over that for zero bias. A preliminary experiment to detect such an increase in the annealing rate (a factor of 9 at 200 K for the values assumed in the text) has given a *negative* result. The zero-bias annealing results may therefore require an alternate explanation.

VI. SUMMARY

We have observed a level at $E_c - 0.45 \text{ eV}$ which arises from isolated interstitial boron in silicon. From DLTS studies of this level and correlation with previously published EPR studies of the photoexcited neutral state, we arrive at the following conclusions:

- (1) Three charge states exist for neutral boron, B_i^+ , B_i^0 , and B_i^- .
- (2) The electrical levels associated with these charge states are inverted from the usual order with the acceptor state ($-/0$) at $E_c - 0.45 \text{ eV}$ and a donor state ($0/+$) above it at $\sim E_c - 0.15 \text{ eV}$. Interstitial boron is, therefore, an example of an Anderson negative- U system, with B_i^0 a *metastable* state.
- (3) Enhanced annealing is observed under minority-carrier injection and results from a Bourgoin saddle-point mechanism between the charge states B_i^+ and B_i^- . The metastable intermediate B_i^0 state seen in EPR allows a detailed microscopic mechanism to be proposed in which the interstitial boron atom moves from a site of $\langle 111 \rangle$ axial symmetry for B_i^+ to one of $\langle 100 \rangle$ -like

symmetry for B_i^- . A possible model consistent with the data is a change from a $\langle 111 \rangle$ bond-centered position to a $\langle 100 \rangle$ -split interstitial, both configurations previously predicted from theoretical considerations. An alternative model with B_i^+ in the normal hexagonal interstitial site and converting to a $\langle 100 \rangle$ -split B_i^- configuration is also a possibility.

The concept of a negative- U was first proposed by Anderson⁸ to explain the properties of amorphous chalcogenide glasses. The extension of this concept to defects was first introduced by Street and Mott.³² Although it is generally accepted that this is indeed probably the correct explanation for the properties of these materials,^{32,33} until now there has been no concrete microscopic identification of any defect in a solid with a negative U .

We believe that the experimental observations described here supply strong evidence that interstitial boron is such a system. In addition, our results demonstrate that, in this case, it is the energy gained by a change in lattice coordination that serves to overcome the Coulomb repulsion energy of the additional electrons.

Recently, Baraff, Kane, and Schlüter³⁴ have suggested on the basis of theoretical considerations that the isolated vacancy in silicon is a negative- U system with V^+ a metastable state between inverted single-donor ($0/+$) and double-donor ($+ / ++$) levels. Our unpublished experimental results for this defect also can be interpreted to confirm their sug-

gestion but the evidence is not yet as strong as those we have presented here for interstitial boron. This is currently under study and has been the subject of a recent preliminary communication.³⁵ If their suggestion is correct, the driving force there must come from the change in the magnitude of a tetragonal Jahn-Teller distortion with no change in symmetry of the defect.

The Bourgoin mechanism for ionization-enhanced defect migration in semiconductors was first proposed in 1972.^{5,7} Again, however, no positive evidence that any defect displayed this effect has been found until the present work.

Interstitial boron, therefore, serves as a unique model system in that it provides an example for the first time of two independent important predicted phenomena: the Anderson negative U and the Bourgoin mechanism. Work is continuing to further elucidate the microscopic processes.

ACKNOWLEDGMENTS

We are indebted to Dr. A. O. Ewvaraye for supplying some of the sample diodes used in this study. Helpful discussions with Dr. L. C. Kimerling are also gratefully acknowledged. One of us (J.R.T.) would like to thank the Sherman Fairchild Foundation for fellowship support. This research was supported by the U. S. Navy ONR Electronics and Solid State Science Program, Contract No. N00014-76-C-1097.

*Present address: Electronics Department, General Motors Research Laboratories, General Motors Technical Center, Warren, Michigan 48090.

¹G. D. Watkins, *Radiation Damage in Semiconductors* (Dunod, Paris, 1964), p. 97.

²G. D. Watkins, *Inst. Phys. Conf. Ser.* **23**, 1 (1975).

³G. D. Watkins, J. R. Troxell, and A. P. Chatterjee, *Inst. Phys. Conf. Ser.* **46**, 16 (1979).

⁴G. D. Watkins, *Phys. Rev. B* **12**, 5824 (1975).

⁵J. C. Bourgoin and J. W. Corbett, *Phys. Lett.* **38A**, 135 (1972).

⁶J. C. Bourgoin and J. W. Corbett, *Radiat. Eff.* **36**, 157 (1978).

⁷Authors in the Soviet literature ([see, e.g., A. E. Kiv and Z. A. Iskanderova, *Fiz. Tekh. Poluprovadn.* **9**, 325 (1975)] [*Sov. Phys. Semicond.* **9**, 211 (1975)]) give credit also to B. L. Oksengendler for this mechanism. The reference cited: B. L. Oksengendler, in *Method of Radiation Interactions in Studies of Structure and Properties of Solids* [in Russian] (FAN, Tashkent, 1971), appears not to be available in the West.

⁸P. W. Anderson, *Phys. Rev. Lett.* **34**, 953 (1975).

⁹D. V. Lang, *J. Appl. Phys.* **45**, 3014 (1974); **45**, 3023 (1974).

¹⁰J. R. Troxell and G. D. Watkins, *Rev. Sci. Instrum.* **51**, 143 (1980).

¹¹The $E(0.16)$ and $E(0.43)$ levels emerge upon annealing at ~ 80 K where the silicon vacancy becomes mobile (unpublished).

¹²L. C. Kimerling, *Inst. Phys. Conf. Ser.* **31**, 221 (1977).

¹³L. C. Kimerling, H. M. DeAngelis, and J. W. Diebold, *Solid State Commun.* **16**, 171 (1975).

¹⁴Olof Engström and Anders Alm, *Solid State Electron.* **21**, 1571 (1978).

¹⁵The notation (i/j) used in this paper means that the defect has charge state i when the level is occupied by an electron, j if unoccupied.

¹⁶P. M. Mooney, L. J. Cheng, M. Suli, J. D. Gerson, and J. W. Corbett, *Phys. Rev. B* **15**, 3836 (1977).

¹⁷A. O. Ewvaraye, *J. Appl. Phys.* **48**, 734 (1977).

¹⁸C. H. Henry, H. Kukimoto, G. L. Miller, and F. R. Merritt, *Phys. Rev. B* **7**, 2499 (1973).

¹⁹L. C. Kimerling, *Solid State Electron.* **21**, 1391 (1978).

²⁰D. V. Lang and L. C. Kimerling, *Phys. Rev. Lett.* **33**, 489 (1974).

²¹L. C. Kimerling and D. V. Lang, *Inst. Phys. Conf. Ser.* **23**, 589 (1975).

²²D. V. Lang, L. C. Kimerling, and S. Y. Leung, *J. Appl. Phys.* **47**, 3587 (1976).

²³D. V. Lang and L. C. Kimerling, *Appl. Phys. Lett.* **28**, 248 (1976).

²⁴J. R. Troxell, A. P. Chatterjee, G. D. Watkins, and

- L. C. Kimerling, *Phys. Rev. B* 19, 5336 (1979).
- ²⁵G. D. Watkins, R. P. Messmer, C. Weigel, D. Peak, and J. W. Corbett, *Phys. Rev. Lett.* 27, 1573 (1971).
- ²⁶C. Weigel, D. Peak, J. W. Corbett, G. D. Watkins, and R. P. Messmer, *Phys. Rev. B* 8, 2906 (1973).
- ²⁷C. Weigel, D. Peak, J. W. Corbett, G. D. Watkins, and R. P. Messmer, *Phys. Status Solidi B* 63, 131 (1974).
- ²⁸G. D. Watkins and K. L. Brower, *Phys. Rev. Lett.* 36, 1329 (1976).
- ²⁹Alison Mainwood, F. P. Larkins, and A. M. Stoneham, *Solid State Electron.* 21, 1431 (1978).
- ³⁰S. M. Sze, *Physics of Semiconductor Devices* (Wiley, New York, 1969).
- ³¹L. C. Kimerling, H. M. DeAngelis, and C. P. Carnes, *Phys. Rev. B* 3, 427 (1971).
- ³²R. A. Street and N. F. Mott, *Phys. Rev. Lett.* 35, 1293 (1975).
- ³³Marc Kastner, David Adler, and H. Fritzsche, *Phys. Rev. Lett.* 37, 1504 (1976).
- ³⁴G. A. Baraff, E. O. Kane, and M. Schlüter, *Phys. Rev. Lett.* 43, 956 (1979).
- ³⁵G. D. Watkins and J. R. Troxell, *Phys. Rev. Lett.* 44, 593 (1980).